Tech Science Press

Green Nanocomposites Made With Polyvinyl Alcohol and Cellulose Nanofibers Isolated From Recycled Paper

Le Van Hai[1,2], Lindong Zhai[1], Hyun Chan Kim[1], Jung Woong Kim[1] and Jaehwan Kim[1,*]

[1]Creative Research Center for Nanocellulose Future Composites, Inha University, Incheon, Republic of Korea.

[2]Department of Pulp and Paper Technology, Phutho College of Industry and Trade, Phutho, Vietnam.

[*]Corresponding Author: Jaehwan Kim. Email: jaehwan@inha.ac.kr.

Abstract: This paper reports green nanocomposites made by blending polyvinyl alcohol (PVA) with cellulose nanofiber (CNF) isolated from recycled deinked copy/printing paper (DIP). The reinforcement effect of DIPCNF in the nanocomposites is compared with other CNFs isolated from native cotton and hardwood by means of TEMPO-oxidation. The prepared PVA-CNF nanocomposites are characterized in terms of morphology, chemical interaction, structural, thermal and mechanical properties. X-ray diffraction and Fourier transform infrared spectroscopy confirm the reinforcing ability of cellulose nanofibers into PVA. By blending CNFs into PVA matrix, the thermal stability of the nanocomposites is improved and DIPCNF shows similar enhancement effect with COCNF and HWCNF. The prepared nanocomposites exhibit 50% Young's modulus improvement by adding 6% of CNF and DIPCNF exhibits similar enhancement of the mechanical properties to COCNF and HWCNF in the nanocomposites. This indicates that the use of DIPCNF is beneficial for environment protection, resource retaining and save energy in comparison with COCNF and HWCNF.

Keywords: Green nanocomposite; cellulose; TEMPO-oxidation; recycled paper, polyvinyl alcohol

1 Introduction

In recent years, eco-friendly green composite materials are concerned to research and industrialization for future products because of pollution, environment, health, safety and depletion of fossil fuel resources. Cellulose is a green material that is biodegradable, biocompatible, non-toxic, low cost and widely available in nature. Cellulose has been mostly used in pulp and paper industries. Recycling products can bring better environmental protection and sustainable resource use. Recently, cellulose nanofibers (CNFs) have gained much attention for various applications due to their superior characteristics in terms of renewability, biodegradability, biocompatibility, high mechanical strength, high elastic modulus, lightweight, low thermal expansion, optical transparency and thermal stability [1-3]. To produce CNFs, different methods are used such as sulfuric acid hydrolysis [4-7], TEMPO oxidation [8-11], and mechanical extraction methods [12-14]. Various cellulose resources are available for isolating CNFs [5-7,10,15]. CNFs have enormous potentials for many different applications such as packaging, paper, plastic, and cement industries [16]. The recycled cellulose used for paper products and packaging is well known for years all over the world. Re-used and recycled resource could offer better environmental protection. Several research groups used recycled cellulose such as recycled deinked copy/printing paper (DIP) for CNF production [17-19]. They applied CNFs for paper, paperboard and nanocomposites.

Reinforcement of CNFs into different polymers gained much attention as it can enhance the mechanical properties, thermal properties of nanocomposites. There are many polymer nanocomposites reinforced by CNFs such as cellulose-cellulose, polyvinyl alcohol (PVA), polyvinyl chloride (PVC), polyethylene (PE) and polypropylene (PP) [20]. Recycle of cellulose for CNFs is a good way to sustain

DOI: 10.32604/jrm.2019.06466

the resource and build up environmentally friendly products. However, the effect of TEMPO-oxidized CNF isolated from recycled resource has not been concerned for especially PVA nanocomposites. Furthermore, there is no detail information on the effect of CNFs isolated from recycled products, on the mechanical, thermal properties of PVA nanocomposites. Thus, this research aims at developing CNF reinforced PVA nanocomposites by considering the effects of recycled CNFs on the properties of nanocomposites. In this research, TEMPO-oxidized CNFs, produced from different cellulose resources namely hardwood, cotton linter and recycled deinked copy/printing paper, are used to develop PVA-CNF nanocomposites using a simple mixing and casting method. Field emission transmission electron microscopy (FETEM) and atomic force microscopy (AFM) were used to investigate the morphology and length-width ratio of cellulose nanofibers.

Properties of the nanocomposites such as thermal degradation, mechanical property, and crystallinity index are important understand their behaviors. Several publications mentioned the thermal degradation and mechanical properties of PVA-CNF nanocomposites that use different CNFs [21-27]. CNF reinforced PVA nanocomposites increased their mechanical properties and thermal stability [28-29]. It is however, none of the previous publications concerned the effect of cellulose nanofiber from recycled source on the PVA nanocomposites. Mechanical and thermal properties of the nanocomposites are investigated by comparing the nanocomposites with the native CNF as well as the pristine PVA polymer. Additionally, crystallinity index is an important factor contributed to the mechanical enhancement of PVA-CNF nanocomposites. In this research, the reinforcement of CNFs in the nanocomposites is studied by taking the XRD to see the effect of crystallinity on the nanocomposites. Especially CNF isolated from DIP is focused in the PVA-CNF nanocomposites research.

2 Materials and Methods

2.1 Materials

Cellulose nanofibers from three different cellulose sources, namely, cotton linter nanofiber (COCNF), mixture bleached hardwood kraft pulp nanofiber (HWCNF) and recycled deinked copy/printing paper nanofiber (DIPCNF) were prepared follow previous work with a little modification for sonication process. Polyvinyl alcohol (Sigma Aldrich, MW 85000-124000, 99%, hydrolysed) was used as purchased.

2.2 Preparation of PVA-CNF Nanocomposites

Cellulose nanofibers from three different cellulose sources were used to prepare PVA-CNF nanocomposites. CNFs were prepared by TEMPO-oxidation [30]. In brief, TEMPO-oxidized cellulose was mechanically disintegrated by using a homogenizer mixer (T25, IKA) for 10 minutes. Homogenous cellulose solution was continually treated by using a sonicator (SONOPLUS 2200, 200 Watt) at 35% power for 10 minutes. PVA-CNF nanocomposites were prepared by a simple casting method. A defined amount of PVA was dissolved in water at 85^{o}C with under magnetic stirring for 3 hours. Then CNF suspension was added in PVA solution according to desired amount and continully stirred for another 1 hour. Mixed solutions were then cast on a petri dish and kept in a calibrated table, followed by drying in a clean condition room. The pristine PVA specimen was also prepared by following the same preparation method for comparison.

2.3 Mechanical Property Test

To measure yield strength and Young's modulus, stress-strain curves of the samples were found by using a tensile test equipment previously reported [31-32]. Samples were kept at 23^{o}C and 50% RH overnight in an environmental chamber that can control temperature and humidity. The samples were cut to the size of 60 × 5 mm for the tensile test. The strength property was evaluated by using the tensile test equipment. The speed of test was set up at 0.05 mm/s. The active length between two grips of the tensile test equipment was 30 mm.

2.4 Characterizations

To investigate the morphology of CNFs, a FETEM (JEM2100F, JEOL) and an AFM (Dimension 3100, Veeco) were used. For the FETEM, a diluted CNFs suspension was prepared on a TEM grid for fiber length and width determination. The grid was dip into the CNF suspension and bottled by Whatman filter paper and air dried. The length-width ratio of CNFs was analyzed by using the imageJ (VJ 1.50i) software [33]. Additionally, CNF suspension was spay-deposited on a silicon wafer for the AFM investigation. An AFM was used in tapping mode to see the morphology of the samples.

To investigate chemical, physical characteristics of the nanocomposites, a Fourier transform infrared spectroscopy (FTIR, Bruker Vertex 80V), thermogravimetric analyzer (TGA, NETZSCH TG 209F3) and an X-Ray diffractometer (XRD, Rigaku RINT2000) were used. For the XRD analysis, the samples were cut to 2 × 2 cm^2 and used for analysis. FTIR was used to define the chemical structure of the PVA and PVA-CNF nanocomposites. The scanning range was from 400 to 4000 cm^{-1}. TGA was carried by using an Al_2O_3 crucible at an atmosphere of dry gas flow. The temperature range was 30 to 600°C and the sample weight was 7 mg. The X-ray was operated at 40 kV/100 mA, scanning range was 5-40° with a step of 0.02°.

3 Results and Discussion

3.1 CNF Morphology

Morphologies of the CNFs were investigated by using AFM and FETEM. Figs. 1(a)-1(c) show the FETEM images of HWCNF, COCNF and DIPCNF. The FETEM images show the manifest of the fiber length. Width values of the CNFs are 13.3 ± 4.0, 13.8 ± 3.8 and 14.7 ± 6.3 nm and the length values are 614 ± 276, 629 ± 260 and 599 ± 241 nm for HWCNF, COCNF, and DIPCNF, respectively. The aspect ratio of CNF is in the range of 41-47. Figs. 1(d)-1(f) show AFM images for HWCNF, COCNF and DIPCNF. The images represent height of CNFs observed by taping modes. The AFM and FETEM images show that CNF isolated from recycled paper offered almost the same morphology as native hardwood and cotton sources. Hence, recycled fiber seems to be a good resource for CNF production and applications.

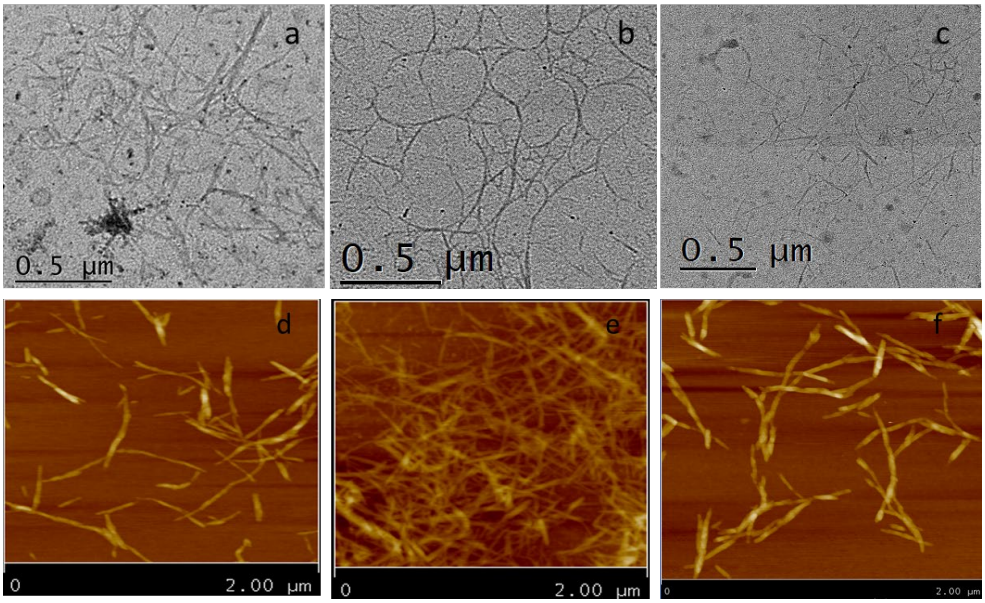

Figure 1: Morphologies of individual CNFs observed by FETEM: (a) HWCNF, (b) COCNF, (c) DIPCNF and by AFM: (d) HWCNF, (e) COCNF, (f) DIPCNF

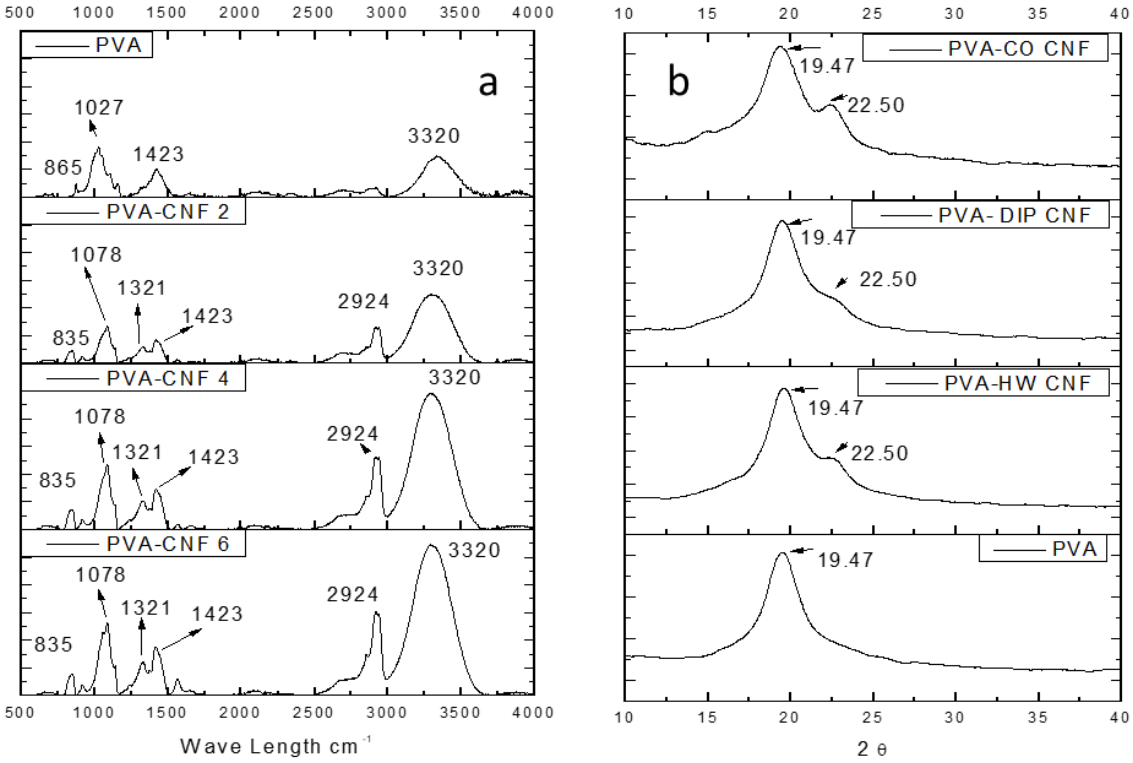

Figure 2: (a) FT-IR of PVA and PVA-DIPCNF nanocomposites with different CNF content and (b) XRD patterns of PVA and PVA-CNF nanocomposites

3.2 FTIR and XRD

Fig. 2(a) shows the FTIR of the pristine PVA and PVA-DIPCNF nanocomposites. The pristine PVA and PVA-DIPCNF nanocomposites with different CNF contents were investigated. The pristine PVA shows peaks at 1027, 1423 cm^{-1} and a board band at 3320 cm^{-1}, which correspond to the C-O stretching, C-C stretching and OH bonded groups, respectively [26,34]. The band peak at 2924 cm^{-1} is assigned to C-H vibration. This peak is appeared when CNF is added to the PVA polymer. The higher absorbance band at 2924 cm^{-1} is shown to be clear when the CNF content is high. Furthermore, the addition of CNF to the PVA shows a high peak at 3320 cm^{-1}, which contributes to the hydrogen bond increase of the PVA-DIPCNF nanocomposites. The peak at 1027 cm^{-1} exhibits a small shift to 1078 cm^{-1}. The intensity of peak at 1150 and 3300 cm^{-1} are shifted up in the PVA-DIPCNF nanocomposites due to hydrogen bonds between CNF and PVA. Additionally, the reinforcement of CNF brought an additional peak at 1321 cm^{-1}. By reinforcing the pristine PVA with CNFs, hydrogen bonds were formed, which improve the properties of PVA-DIPCNF nanocomposite. The FTIR results prove the hydrogen bond formation in the PVA-DIPCNF nanocomposite.

Fig. 2(b) shows the XRD patterns of the pristine PVA and PVA-CNF nanocomposites. The pristine PVA shows a peak at 19°. Addition of CNF in the PVA polymer resulted in another peak at 22°, which corresponds to the crystalline peak of cellulose. From the XRD pattern, the appearance of additional peak at 22° confirms the successful reinforcement of CNF in the PVA polymer. Note that the peak intensity at 22° for PVA-DIPCNF is slightly weaker than that of PVA-HWCNF and PVA-COCNF. As COCNF has high crystallinity index, PVA-COCNF has the highest peak intensity at 22°.

3.3 Thermal Analysis

Thermal degradation of the PVA-CNF nanocomposites is shown in Fig. 3 with different CNFs: HWCNF, COCNF and DIPCNF. The number appeared after PVA-CNF indicates the weight percent of CNF. The thermal degradation of the pristine PVA starts at 225°C and approached to 300°C. The PVA-DIPCNF nanocomposite shows better thermal stability than others. At 255°C, 45% weight loss is shown for the pristine PVA and PVA-DIPCNF2. Also, at this temperature, only 34 and 29% weight losses are observed for PVA-DIPCNF4 and PVA-DIPCNF6, respectively. Tab. 1 shows the summary of the TGA results. Further at 220 to 290°C, 68% weight loss was observed for the pristine PVA, meanwhile 62, 57 and 53% for 2, 4 and 6% DIPCNF reinforced PVA nanocomposites, respectively. The weight losses of PVA-COCNF nanocomposite at 220-290°C, are shown to be 68, 60 and 71% for the addition of 2, 4 and 6% COCNFs, respectively. In the case of PVA-HWCNF, the weight losses are 60, 61 and 57% for PVA-HWCNF2, PVA-HWCNF4 and PVA-HWCNF6 at 220-290°C, respectively.

The thermal degradation analysis shows that the addition of CNFs into PVA matrix enhances the thermal stability of the nanocomposites. Note that DIPCNF shows similar enhancement in the thermal stability with COCNF and HWCNF. It indicates that the recycled fiber source has positive effect on the thermal stability of DIPCNF to PVA nanocomposites. It should be concluded that PVA-DIPCNF does not show better thermal stability than PVA-HWCNF and PVA-COCNF.

Table 1: TGA results of PVA and PVA-CNF nanocomposites

	Water evaporation stage (100°C)	Weight loss (%) at (100-220°C)	Weight loss (%) at (220-290°C)	Weight loss (%) at (290-390°C)
PVA	5	9	68	73
PVA-HWCNF2	5	9	60	68
PVA-HWCNF4	5	9	61	71
PVA-HWCNF6	5	9	57	72
PVA-COCNF2	5	11	68	74
PVA-COCNF4	5	10	60	71
PVA-COCNF6	5	14	71	82
PVA-DIPCNF2	5	10	62	67
PVA-DIPCNF4	5	8	57	73
PVA-DIPCNF6	5	9	53	71

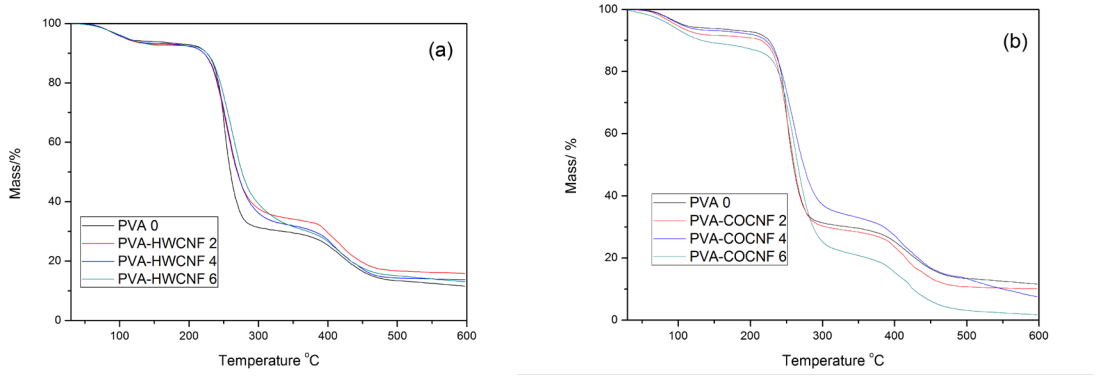

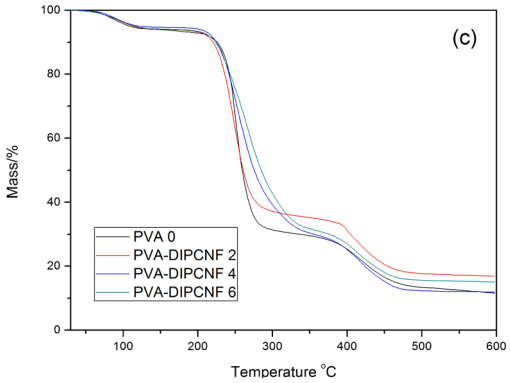

Figure 3: Thermal degradation of PVA-CNF nanocomposites: (a) HWCNF, (b) SWCNF and (c) DIPCNF

3.4 Mechanical Properties

Fig. 4 shows stress and strain curves of the pristine PVA and PVA-CNF nanocomposites. Tab. 2 presents their mechanical properties. Young's modulus of PVA-CNF nanocomposites increased quickly with the addition of CNFs to the pristine PVA. In detail, 2-6% addition of CNFs to the pristine PVA resulted in a noticeable enhancement in Young's modulus from 5% to 50%. Nanocomposites reinforced with recycled cellulose source showed similar effect to native cellulose nanofibers (HWCNF and COCNF). The tensile strength and Young's modulus of PVA-CNF increased, and the highest improvement of PVA-CNF nanocomposites was shown by the reinforcement of COCNF. In the case of HWCNF and DIPCNF, the results showed similar tensile strength improvement. However, the PVA-DIPCNF showed better improvement for Young's modulus. One important point is that CNF from recycled paper (DIPCNF) also showed similar performance as native cellulose resources. DIP-CNF, HW-CNF and CO-CNF offered almost the same reinforced properties in terms of tensile strength and thermal stability. The use of recycled cellulose source can offer more environmentally friendly product without sacrificing mechanical properties and maintaining cost effectiveness. Although PVA-DIPCNF does not offer better mechanical improvement than PVA-HWCNF and PVA-COCNF, the use of DIPCNF is beneficial for environment protection, resource retaining and save energy. In other words, the use of recycled paper for green nanocomposite fabrication offers environment protection and sustainable resources with low cost.

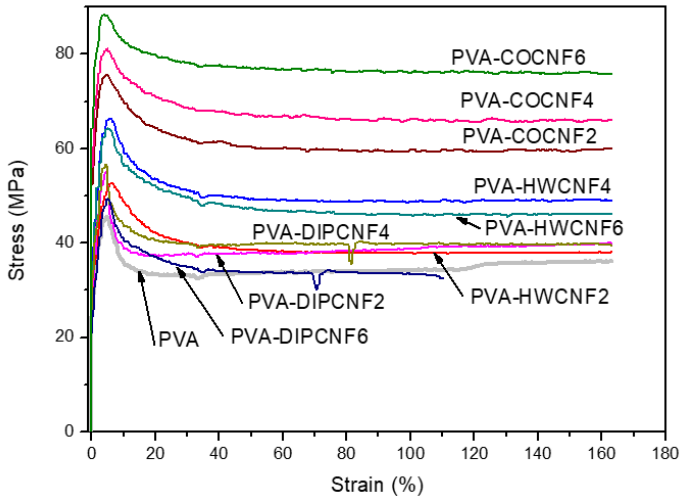

Figure 4: Stress-strain curves of PVA-CNF nanocomposites

Table 2: Mechanical properties of PVA-CNF nanocomposites

Sample name	Yield strength (MPa)	Young's modulus (GPa)	Young's modulus increase (%)
PVA	46.6 ± 5.7	1.83 ± 0.15	0.0
PVA-HWCNF2	51.9 ± 3.2	1.92 ± 0.16	5.1
PVA-HWCNF4	55.7 ± 2.3	2.08 ± 0.05	13.8
PVA-HWCNF6	55.5 ± 4.6	2.32 ± 0.52	27.0
PVA-COCNF2	73.5 ± 7.3	2.48 ± 0.29	35.2
PVA-COCNF4	75.9 ± 9.0	2.49 ± 0.26	35.9
PVA-COCNF6	77.3 ± 7.3	2.78 ± 0.45	51.8
PVA-DIPCNF2	55.3 ± 1.3	2.15 ± 0.06	17.5
PVA-DIPCNF4	55.8 ± 3.3	2.24 ± 0.02	22.2
PVA-DIPCNF6	50.2 ± 6.6	2.51 ± 0.34	37.3

3.5 Morphology of PVA-CNF Nanocomposites

Morphologies of PVA and PVA-DIPCNF nanocomposite was investigated by using the FESEM S-4000. The surface and cross-section SEM images of the nanocomposite are shown in Fig. 5. Surface structures of the PVA and PVA-DIPCNF did not show clear difference between them. Note that the PVA and PVA nanocomposite show smooth surfaces. However, the cross-section SEM images of the PVA and PVA-DIPCNF nanocomposite show difference. The PVA exhibits less porosity meanwhile PVA-DIPCNF reveals more porosity in their cross-sections. Thus, the PVA-DIPCNF nanocomposite exhibits less compact structure than the PVA. Furthermore, the PVA-DIPCNF represents less tensile strength improvement than that of HWCNF and COCNF cases. It might be due to low crystallinity of DIPCNF. The low crystallinity of DIPCNF results in less reinforcing behavior of DIPCNF in the nanocomposites. As a result, the PVA-DIPCNF case shows the lowest improvement of tensile strength in comparison with the HWCNF and COCNF cases as shown in Tab. 2.

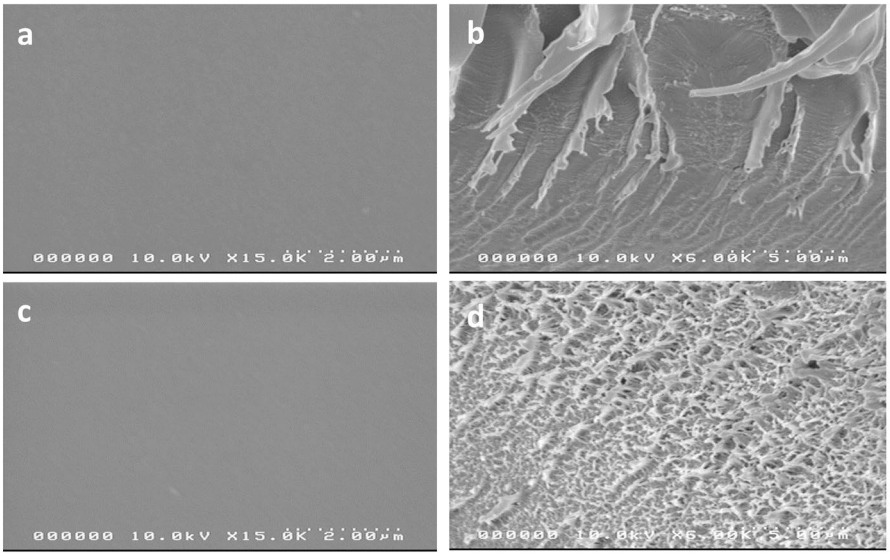

Figure 5: SEM images: (a) Surface of PVA, (b) cross section of PVA, (c) surface of PVA-DIPCNF nanocomposite and (d) cross section of PVA-DIPCNF nanocomposite

4 Conclusions

Green PVA-CNF nanocomposites were fabricated by blending PVA and CNFs isolated from recycled deinked copy/printing paper (DIP). The reinforcement effect of DIPCNF in the nanocomposites was compared with other CNFs isolated from native cotton and hardwood by means of TEMPO-oxidation. The AFM and FETEM analysis showed that DIPCNF offered almost the same morphology as CNFs from native hardwood and cotton sources. XRD and FTIR results confirmed the successful reinforcement of CNFs in PVA polymer. Thermal degradation analysis showed that the addition of CNFs into PVA matrix enhanced the thermal stability of the nanocomposites. In comparison of CNFs effect, DIPCNF showed similar enhancement effect of the thermal stability with COCNF and HWCNF.

The higher the loading of CNFs into the PVA matrix exhibited the better the tensile strength and Young's modulus. The Young's modulus of PVA-CNF nanocomposites presented 5-50% improvement from the pristine PVA. DIPCNF showed similar enhancement of the mechanical properties to COCNF and HWCNF in the PVA-CNF nanocomposites. This indicates that although PVA-DIPCNF does not offer better mechanical improvement of the nanocomposites than PVA-HWCNF and PVA-COCNF, the use of DIPCNF is beneficial for environment protection, resource retaining and save energy.

Acknowledgement: This research was supported by Inha University Research Fund.

References

1. John, M. J., Anandjiwala, R. D., Pothan, L. A., Thomas, S. (2007). Cellulosic fibre-reinforced green composites. *Composite Interfaces, 14(7-9),* 733-751.
2. Kim, J. H., Shim, B. S., Kim, H. S., Lee, Y. J., Min, S. K. et al. (2015). Review of nanocellulose for sustainable future materials. *International Journal of Precision Engineering and Manufacturing-Green Technology, 2(2),* 197-213.
3. Takagi, H., Nakagaito, A. N., Bistamam, M. S. A. (2013). Extraction of cellulose nanofiber from waste papers and application to reinforcement in biodegradable composites. *Journal of Reinforced Plastics and Composites, 32(20),* 1542-1546.
4. Dong, X. M., Kimura, T., Revol, J. F., Gray, D. G. (1996). Effects of ionic strength on the isotropic-chiral nematic phase transition of suspensions of cellulose crystallites. *Langmuir, 12(8),* 2076-2082.
5. Camacho, M., Ureña, Y. R. C., Lopretti, M., Carballo, L. B., Moreno, G. et al. (2017). Synthesis and characterization of nanocrystalline cellulose derived from pineapple peel residues. *Journal of Renewable Materials, 5(3-4),* 271-279.
6. Helbert, W., Cavaille, J. Y., Dufresne, A. (1996). Thermoplastic nanocomposites filled with wheat straw cellulose whiskers. Part I: processing and mechanical behavior. *Polymer Composites, 17(4),* 604-611.
7. Hai, L. V., Seo, Y. B. (2017). Characterization of cellulose nanocrystal obtained from electron beam treated cellulose fiber. *Nordic Pulp & Paper Research Journal, 32(2),* 170-178.
8. Fukuzumi, H., Saito, T., Isogai, A. (2013). Influence of TEMPO-oxidized cellulose nanofibril length on film properties. *Carbohydrate Polymers, 93(1),* 172-177.
9. Isogai, A., Saito, T., Fukuzumi, H. (2011). TEMPO-oxidized cellulose nanofibers. *Nanoscale, 3(1),* 71-85.
10. Saito, T., Kimura, S., Nishiyama, Y., Isogai, A. (2007). Cellulose nanofibers prepared by TEMPO-mediated oxidation of native cellulose. *Biomacromolecules, 8(8),* 2485-2491.
11. Hai, L. V., Zhai, L., Kim, H. C., Kim, J. W., Choi, E. S. et al. (2018). Cellulose nanofibers isolated by TEMPO-oxidation and aqueous counter collision methods. *Carbohydrate Polymers, 191,* 65-70.
12. Abraham, E., Deepa, B., Pothan, L. A., Jacob, M., Thomas, S. et al. (2011). Extraction of nanocellulose fibrils from lignocellulosic fibres: a novel approach. *Carbohydrate Polymers, 86(4),* 1468-1475.
13. Besbes, I., Vilar, M. R., Boufi, S. (2011). Nanofibrillated cellulose from alfa, eucalyptus and pine fibres: preparation, characteristics and reinforcing potential. *Carbohydrate Polymers, 86(3),* 1198-1206.
14. Le Van Hai, Seo, Y. B. (2018). Properties of nanofibrillated cellulose prepared by mechanical means. *Cellulose Chemistry and Technology, 52(9-10),* 741-747.

15. Joy, J., Jose, C., Varanasi, S. B., Mathew, P., Thomas, S. et al. (2016). Preparation and characterization of poly (butylene succinate) bionanocomposites reinforced with cellulose nanofiber extracted from Helicteres isora plant. *Journal of Renewable Materials, 4(5),* 351-364.
16. Cowie, J., Bilek, E. T., Wegner, T. H., Shatkin, J. A. (2014). Market projections of cellulose nanomaterial-enabled products-Part 2: Volume estimates. *TAPPI Journal, 13(6),* 57-69.
17. Danial, W. H., Majid, Z. A., Muhid, M. N. M., Triwahyono, S., Bakar, M. B. et al. (2015). The reuse of wastepaper for the extraction of cellulose nanocrystals. *Carbohydrate Polymers, 118,* 165-169.
18. Filson, P. B., Dawson-Andoh, B. E., Schwegler-Berry, D. (2009). Enzymatic-mediated production of cellulose nanocrystals from recycled pulp. *Green Chemistry, 11(11),* 1808-1814.
19. Wang, H., Li, D., Zhang, R. (2013). Preparation of ultralong cellulose nanofibers and optically transparent nanopapers derived from waste corrugated paper pulp. *BioResources, 8(1),* 1374-1384.
20. Azizi Samir, M. A. S., Alloin, F., Dufresne, A. (2005). Review of recent research into cellulosic whiskers, their properties and their application in nanocomposite field. *Biomacromolecules, 6(2),* 612-626.
21. Li, W., Wu, Q., Zhao, X., Huang, Z., Cao, J. et al. (2014). Enhanced thermal and mechanical properties of PVA composites formed with filamentous nanocellulose fibrils. *Carbohydrate Polymers, 113,* 403-410.
22. Lu, J., Wang, T., Drzal, L. T. (2008). Preparation and properties of microfibrillated cellulose polyvinyl alcohol composite materials. *Composites Part A: Applied Science and Manufacturing, 39(5),* 738-746.
23. Miao, J., Zhang, R., Bai, R. (2015). Poly (vinyl alcohol)/carboxymethyl cellulose sodium blend composite nanofiltration membranes developed via interfacial polymerization. *Journal of Membrane Science, 493,* 654-663.
24. Niu, Y., Zhang, X., He, X., Zhao, J., Zhang, W. et al. (2015). Effective dispersion and crosslinking in PVA/cellulose fiber biocomposites via solid-state mechanochemistry. *International Journal of Biological Macromolecules, 72,* 855-861.
25. Sun, X., Lu, C., Liu, Y., Zhang, W., Zhang, X. (2014). Melt-processed poly (vinyl alcohol) composites filled with microcrystalline cellulose from waste cotton fabrics. *Carbohydrate Polymers, 101,* 642-649.
26. Voronova, M. I., Surov, O. V., Guseinov, S. S., Barannikov, V. P., Zakharov, A. G. (2015). Thermal stability of polyvinyl alcohol/nanocrystalline cellulose composites. *Carbohydrate Polymers, 130,* 440-447.
27. Bhatnagar, A., Sain, M. (2005). Processing of cellulose nanofiber-reinforced composites. *Journal of Reinforced Plastics and Composites, 24(12),* 1259-1268.
28. Cai, J., Chen, J., Zhang, Q., Lei, M., He, J. et al. (2016). Well-aligned cellulose nanofiber-reinforced polyvinyl alcohol composite film: mechanical and optical properties. *Carbohydrate Polymers, 140,* 238-245.
29. Ren, L. Z., Ren, P. G., Zhang, X. L., Sun, Z. F., Zhang, Y. (2014). Preparation and mechanical properties of regenerated cellulose/poly (vinyl-alcohol) physical composite hydrogel. *Composite Interfaces, 21(9),* 853-867.
30. Isogai, A., Kato, Y. (1998). Preparation of polyuronic acid from cellulose by TEMPO-mediated oxidation. *Cellulose, 5(3),* 153-164.
31. Abas, Z., Kim, H. S., Zhai, L., Kim, J. (2015). Experimental study of vibrational energy harvesting using electro-active paper. *International Journal of Precision Engineering and Manufacturing, 16(6),* 1187-1193.
32. Yun, S., Kim, J., Lee, K. S. (2010). Evaluation of cellulose electro-active paper made by tape casting and zone stretching methods. *International Journal of Precision Engineering and Manufacturing, 11(6),* 987-990.
33. Le Van, H. (2017). Properties of nano-fibrillated cellulose and its length-width ratio determined by a new method. *Cellulose Chemistry and Technology, 51(7-8),* 649-653.
34. Priya, B., Gupta, V. K., Pathania, D., Singha, A. S. (2014). Synthesis, characterization and antibacterial activity of biodegradable starch/PVA composite films reinforced with cellulosic fibre. *Carbohydrate Polymers, 109,* 171-179.